Dalton Transactions

Accepted Manuscript

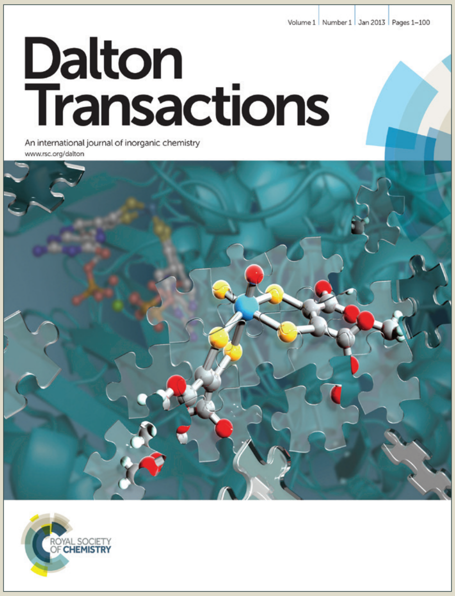

ROYAL SOCIETY OF CHEMISTRY

www.rsc.org/dalton

Exfoliation of one-dimensional TiO_5 chain in K_2TiO_3

Yuji Masubuchi*, Ryo Miyazaki, Hiroki Kikuchi, Teruki Motohashi, Shinichi Kikkawa

Affiliation: Faculty of Engineering, Hokkaido University, N13 W8, Kita-ku, Sapporo, Hokkaido 060-8628, Japan

*Corresponding author: Y. Masubuchi; address: Faculty of Engineering, Hokkaido University, N13 W8, Kita-ku, Sapporo 060-8628, Japan; Tel/Fax: +81-(0)11-706-6742/6740; E-mail: yuji-mas@eng.hokudai.ac.jp

TOC Text

Potassium titanate, K_2TiO_3, was exfoliated in acid solution, and Tyndall scattering due to the colloid formation was observed.

TOC graphic

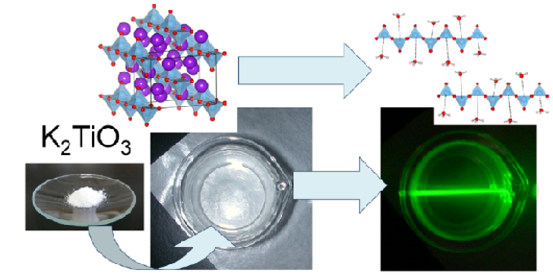

Abstract

Potassium titanate, K_2TiO_3, with a chain structure of TiO_5 polyhedra was exfoliated in an aqueous nitric acid solution of pH ≤ 1 and Tyndall scattering due to the colloid formed by the exfoliation was observed. The colloidal particle size measured by dynamic light scattering was approximately 300 nm. Stripe pattern observed in transmission electron microscopy for the aggregated grains after their drying suggested the TiO_5 chains were exfoliated in acid solution. X-ray absorption showed that the coordination polyhedron around Ti^{4+} changed from a square pyramid in K_2TiO_3 powder to a distorted octahedron formed with the additional hydronium ions in the acidic solution.

1. Introduction

Ion exchange reactions of inorganic oxides with a tunnel or layer structure are attractive chemical processes for creating novel functional materials.[1,2] Cathode materials for lithium ion batteries have been prepared from transition metal oxides with a tunnel structure.[3,4] Inorganic-organic hybrid materials have also been obtained through ion exchange reactions.[5-8] Recently, ion exchange reactions have been further developed to prepare nanoscale materials, such as nanosheets and nanoparticles. Many transition metal oxide and hydroxide nanosheets have been prepared through ion exchange and exfoliation reactions of layer compounds with organic molecules, such as tetrabutylammonium.[9-11] Single crystalline nanosheets are promising precursors for the construction of nanostructured materials, such as multilayer thin films, nanotubes and nanoparticles.[12-16] Parent compounds that exfoliate into nanosheets typically have a two-dimensional layer structure interleaved with alkali cations. However, ion exchange reactions of one-dimensional chain structures have not yet been reported. An exfoliated one-dimensional chain structure is expected to serve as a new building unit for various types of nanostructures similar to nanosheets and also mechanical reinforcement like carbon nanotube.

Potassium titanates with the general formula of $K_2Ti_nO_{2n+1}$ (n = 1 to 8) have chain, layer and tunnel TiO_2 anionic frameworks that interleave K^+ ions, depending on the n-values.[17-21] $K_2Ti_4O_9$ has exchangeable K^+ ions in the interlayers of $(Ti_4O_9)^{2-}$. The potassium cation can be replaced to form $H_2Ti_4O_9•H_2O$ by the ion exchange reaction of $K_2Ti_4O_9$ in diluted HCl. Bronze-type TiO_2 is obtained by the dehydration of $H_2Ti_4O_9•H_2O$ through $H_2Ti_8O_{17}$ with a tunnel structure.[21,22] $H_2Ti_4O_9•H_2O$ reacts further with ethylammonium or tetrabutylammonium hydroxide to exfoliate each TiO_2 layer into nanosheets stabilized by tetrabutylammonium ions in water.[23,24] These nanosheets have been investigated as possible photocatalysts, lithium ion intercalation hosts, and high-κ dielectric materials.[23-26] Potassium monotitanate, K_2TiO_3 with n = 1 in $K_2Ti_nO_{2n+1}$, has the K_2SnO_3 and K_2ZrO_3 related structure crystallized in the *Cmcm* space group, as shown in Fig. 1. K_2TiO_3 consists of chains of *trans* edge-sharing TiO_5 rectangular pyramids with alternating apical directions with potassium ions interleaved between the chains.[17] However, there has been no report to date on the ion exchange properties of K_2TiO_3 in an acid solution. We have recently investigated the intercalation of cisplatin into $K_2Ti_nO_{2n+1}$ with n = 1 and 4 for anticancer drug delivery application.[28] Among the series of potassium titanates, only K_2TiO_3 was found to easily form a transparent colloidal solution in aqueous acid solution. The ion exchange reaction of K_2TiO_3 having a one-dimensional chain structure was thought to exfoliate K_2TiO_3 to nanochains of TiO_5 polyhedra, similar to nanosheets from layered $K_2Ti_4O_9$. To our knowledge, this is the first report on ion exchange and exfoliation of acid-soluble titanium oxide. In this study, the particle size distribution, zeta potential, and the Ti local structure of K_2TiO_3 dispersed in aqueous nitric acid solution were investigated to clarify the exfoliation mechanism and the structure of colloid in acid solution. One-dimensional chain was confirmed by using TEM after its drying.

2. Experimental section

2.1. Synthesis

K_2TiO_3 was prepared by the solid-state reaction of KNO_3 (99.0%, Kanto Chemical) and TiO_2 (>98.0%, Kanto Chemical). These powders were mixed in a molar ratio of K:Ti = 2~2.3:1 with acetone in an agate mortar. The mixed powder was calcined at 850 °C for 20 h in an alumina crucible. Pure K_2TiO_3 was obtained from a mixture of KNO_3/TiO_2 in a molar ratio of 2.2/1 at 850 °C for 20 h due to potassium loss during the reaction, as shown in Fig. S1 of the Supporting Information (SI). The observed lattice parameters were a = 1.0051(4) nm, b = 0.6955(1) nm, and c = 0.5444(6) nm. They are comparable with the reported values of a = 1.0028 nm, b = 0.6935 nm, and c = 0.5453 nm for single crystal K_2TiO_3.[17] Scanning electron microscopy (SEM; JSM-6390LV, Jeol) observations showed an agglomeration of small (<1 μm) particles (see Fig. S2 in SI). K_2TiO_3 powder is extremely hygroscopic and decomposes to an amorphous powder within a few minutes of air exposure. Therefore, the obtained powders were stored in a glovebox filled with dry nitrogen gas until the subsequent dissolution experiment. Approximately 1 mmol (0.174 g) of the obtained powder was dispersed in 100 mL of aqueous 1 M HNO_3 solution in air to obtain a colloidal solution with a Ti concentration of 10 mmol/L.

2.2. Characterization

The crystal phases were characterized using powder X-ray diffraction (XRD; Ultima IV, Rigaku). An air-tight sample holder filled with N_2 gas was used for XRD measurements of the moisture-sensitive K_2TiO_3 powder. The particle size distribution of the Ti colloidal solution was measured using dynamic light scattering (FDLS-3000, Otsuka Denshi) with the detectable range of 0.5 nm ~ 5 μm. The scattered light intensity was plotted along the particle size to study its distribution. The zeta potential of the colloid solution was examined using a zeta potential analyzer (Delsa Nano HC, Beckman Coulter). Microstructure of the colloidal particle was observed by transmission electron microscopy (TEM; JEM-2010, Jeol). A droplet of the solution was supported on a micro-grid coated copper mesh. Chemical composition of the solution separated by filtration was analyzed to study its ion exchange behavior by using inductively coupled plasma-atomic emission spectroscopy (ICP-AES; ICPE-9000, Shimadzu). Ti K-edge X-ray absorption was measured for K_2TiO_3 powder and the Ti colloidal solution in a thin polyethylene bag using the fluorescence mode at the BL-9C beamline of the Photon Factory, High Energy Accelerator Research Organization (KEK), Tsukuba. Extended X-ray absorption fine structure (EXAFS) data were analyzed using the REX2000 software (Rigaku).[29]

3. Results and discussion

K_2TiO_3 powder was dispersed in nitric acid solution with pH ≤ 1. The initial solution was a suspension that became clear and transparent after 3 days. The transparent solution exhibited Tyndall scattering for a green laser, as shown in Fig. 2. Dynamic light scattering was applied to measure the particle size distribution in the colloidal solution. The initial solution had a maximum particle size of about 800 nm, which tailed toward larger particle size, as depicted in Fig. 3. The measured particle size was comparable to that for the starting K_2TiO_3 powder observed using SEM. The particle size did not change significantly over 2 days, but abruptly decreased to a maximum of ca. 300 nm within 3 days and remained constant. The particles with sizes of ca. 300 nm exhibited Tyndall scattering under green laser irradiation (wavelength $\approx$ 532 nm), although the colloidal solution was transparent to the naked eye. The zeta potential of the colloidal solution changed with time, as shown in Fig. S3 (SI), which supports the observed change in particle size. The zeta potential was almost 0 mV for the initial solution until it steeply increased to 30 mV within 3 days. The changes in both particle size and zeta potential at around 3 days may be related to the structural changes during an ion exchange reaction. Potassium ion released to the acid solution was analyzed by ICP-AES. The amount of K^+ increased with duration time and was saturated in 3 days as well as the colloidal particle size and zeta potential as shown in Fig. S4. The extraction behavior was very similar to $K_2Ti_4O_9$ (n=4 in $K_2Ti_nO_{2n+1}$) with layer structure. It was necessary to disperse it in acid solution for several days to remove potassium ions completely from the titanate.[2] Potassium ions in K_2TiO_3 (n = 1) may also be completely exchanged with hydronium ions over a couple of days, as reported for $K_2Ti_4O_9$. K_2TiO_3 was exfoliated to TiO_3^{2-} chains with smaller colloidal size than the parent oxide particles during the reaction with nitric acid. In addition, the zeta potential was increased by the hydration of hydronium ions to the TiO_3^{2-} chains.

Microstructure of the colloidal particle was observed on its dried specimen supported on a copper grid by TEM. The particles of the corrugated chains aggregated into several hundreds of nm grains as shown in Fig. 4(a). The grains almost consisted of titanium oxide, but potassium element hardly appeared in its EDX spectra. Stripe pattern assigned for the chain was obviously observed in the magnified image (Fig. 4(b)). Width of each stripe was below 1 nm which is comparable with length of *b*-axis (0.7 nm) corresponding to the distance between single TiO_5 chains. Electron diffraction of the grains showed an amorphous nature as shown in Fig. 4(c). It was not easy to observe the TiO_5 straight chain structure in nanometer size directly. It may be present in the solution which cannot be applied to the direct observation in TEM apparatus in vacuum. However, the dried grains having a streaked morphology implies an exfoliation reaction of K_2TiO_3 to TiO_5 nanochain structure.

Ti K-edge X-ray absorption near edge structure (XANES) spectra were measured for the K_2TiO_3 powder and colloidal solution after 4 days to elucidate the exfoliation mechanism and structure of K_2TiO_3 in the acid solution. The spectra have large pre-edge peaks at 4967 and 4969 eV for K_2TiO_3 and the acid solution of K_2TiO_3, respectively, as shown in Fig. S5. The relatively strong pre-edge peak suggests that Ti^{4+} ions in the colloid solution are in non-centrosymmetric coordination, similar to a pyramidal structure.[30,31] The pre-edge peak appeared at the same energy as that observed for rutile, which suggests some similarity to the octahedral coordination. The change in coordination with exfoliation is supported by Fourier transforms of the Ti K-edge EXAFS, as shown in Fig. 5. Both the first and second peaks, which correspond to the interatomic distances of Ti-O and Ti-Ti, respectively, are shifted to longer distance in the colloid solution. Ti^{4+} in pyramidal polyhedra was also coordinated together by hydronium ions to form quasi-octahedral environment.

K_2TiO_3 has a one-dimensional chain structure of TiO_5 pyramidal polyhedra with interleaving potassium ions, as shown in Fig. 6(a). When K_2TiO_3 is dispersed in the nitric acid solution, the potassium ions are completely exchanged to hydronium ions, while the TiO_5 chain structure of K_2TiO_3 is maintained (Fig. 6(b)), and the solution gradually becomes clear in several days to exhibit the Tyndall effect depicted in Figs. 2(b) and 2(c). In contrast to the dispersion in acid solution, the K_2TiO_3 did not exfoliate in distilled water (pH = 7). However, the pH value of a suspension of the insoluble white K_2TiO_3 powder increased from 7 to 10. X-ray fluorescence spectroscopy showed a decrease of the K/Ti ratio for the insoluble precipitate powder from 2/1 in K_2TiO_3 to approximately 1/3 for K_2TiO_3 in acid solution. Taking hydronium ions into the TiO_3^{2-} chain structure from solution increased the pH value of the solution and the release of interchain potassium ions from the parent structure, which decreased the K/Ti ratio of the white precipitate. Both the partially decomposed white precipitate and K_2TiO_3 powder exposed in air were XRD amorphous and did not turn to transparent even when they were dispersed in acid solution. The TiO_5 chain structure has already been destroyed before the dispersion. The colloidal particle size in the initial acid solution was almost comparable to that for K_2TiO_3 powder, even after the ion exchange reaction of K_2TiO_3 in aqueous acidic solution had begun, because the residual potassium ions can maintain the network of the chain structure (Fig. 6(b)). After the ion exchange reaction was completed in several days, the parent crystal structure was disrupted into each chain unit, which resulted in a smaller colloidal particle size, as observed in the particle size distribution measurement. However, the chain structure of titanium polyhedra remained even in the solution and exhibited an isomorphic radial distribution function (RDF) calculated from the EXAFS before and after the dispersion in acid solution, as shown in Fig. 6(c). TEM observation also exhibited the trace of chain structure. Each chain unit may be coordinated by hydronium ions to stabilize the chain units in the aqueous solution. Negatively poled oxide ion of H_3O^+ is expected to coordinate additionally to Ti^{4+} polyhedral center. This is quite different from the preparation of nanosheets using bulky organic ions of surfactants. The coordination of H_3O^+ results in an increase in the coordination number, as expected from the XANES spectrum, and also in the interatomic distances, as apparent in the RDF. Hydronium ion exchanged with potassium or sodium ion has been reported on several kinds of layered oxides, such as titanoniobate and mica.[32-34] The increase in zeta potential may be related to the coordination of hydronium ions to the chain structure.

4. Conclusion

Colloid formation was found out on K_2TiO_3 titanate with the structure of rectangular pyramidal TiO_5 polyhedra linked chains. The titanate chains were exfoliated in an aqueous nitric acid solution with pH ≤ 1 and the solution exhibited Tyndall scattering. The RDF around Ti^{4+} calculated from the EXAFS spectrum for the acid solution was very similar to that for the parent K_2TiO_3 powder. TEM observation showed stripe pattern of the exfoliated TiO_5 nanochain structure. Exfoliation in an acid solution may be initiated by ion exchange reaction between K^+ and H_3O^+, so that the solution becomes clear while retaining the chain structure of TiO_5 polyhedra to exhibit Tyndall scattering. The colloidal dispersion of titanium oxide would be very useful as a titanium source for the preparation of functional materials using an aqueous solution route.

Acknowledgment

X-ray absorption measurements were conducted under the approval of the Photon Factory Advisory Committee (Proposal No. 2010G024).

References

(1) W. A. England, J. B. Goodenough, and P. J. Wiseman, *J. Solid State Chem.*, 1983, **49**, 289-299.

(2) H. Izawa, S. Kikkawa, and M. Koizumi, *J. Phys. Chem.*, 1982, **86**, 5023-5026.

(3) Y. Kadoma, S. Oshitari, K. Ui, and N. Kumagai, *Electrochimi. Acta*, 2007, **53**, 1697-1702.

(4) T. Matsumura, R. Kanno, Y. Inaba, Y. Kawamoto, and M. Takano, *J. Electrochem. Soc.*, 2002, **149**, A1509-A1513

(5) S. Kikkawa and M. Koizumi, *Mater. Res. Bull.*, 1980, **15**, 533-539

(6) Z. Tong, T. Shichi, K. Oshika, and K. Takagi, *Chem. Lett.*, 2002, **31**, 876-877.

(7) E. D. Dimotakis, and T. J. Pinnavaia, *Inorg. Chem.*, 1990, **29**, 2393-2394.

(8) H. Tamura, J. Chiba, M. Ito, T. Takeda, and S. Kikkawa, *Solid State Ionics*, 2004, **172**, 607-609.

(9) T. Sasaki, M. Watanabe, H. Hashizume, H. Yamada, and H. Nakazawa, *J. Am. Chem. Soc.*, 1996, **118**, 8329-8335

(10) T. Sasaki, *J. Ceram. Soc. Jpn.*, 2007, **115**, 9-16.

(11) S. Ida, Y. Okamoto, M. Matsuka, H. Hagiwara, and T. Ishihara, *J. Am. Chem. Soc.*, 2012, **134**, 15773-15782.

(12) K. Akatsuka, M. Haga, Y. Ebina, M. Osada, K. Fukuda, and T. Sasaki, *ACS Nano*, 2009, **3**, 1097-1106.

(13) H. Pan, X. Kong, P. Wen, T. Kitayama, and Q. Feng, *Mater. Res. Bull.*, **47** (2012) 2428-2436.

(14) J. Fu, Y. Tian, B. Chang, G. Li, F. Xi, and X. Dong, *J. Solid State Chem.*, 2012, **196**, 282-287.

(15) M. Weia, Y. Konishia, H. Zhoua, H. Sugiharaa, and H. Arakawa, *Solid State Comm.*, 2005, **133**, 493-497.

(16) G. B. Saupe, C. C. Waraksa, H.-N. Kim, Y. J. Han, D. M. Kaschak, D. M. Skinner, and T. E. Mallouk, *Chem. Mater.*, 2000, **12**, 1556-1562.

(17) H. S. Khalsa, M. D. Smith, and H.-C zur Loye. *Mater. Res. Bull.,* 2009, **44**, 91-94.

(18) M. Dion, Y. Piffard, and M. *J.* Tournoux, *Inorg. Nucl. Chem.,* 1978, **40**, 917-918.

(19) T. Shimizu, H. Yanagida, S. Onitsuka, K. Hashimoto, and Y. Nishikawa, *J. Ceram. Soc. Jpn.,* 1981, **89**, 633-635.

(20) H. Cid-Dresdner, and M. J. Buerger, *Z. Kristallogr.,* 1962, **11**, 411-430.

(21) T. Sasaki, M. Watanabe, Y. Fujiki, Y. Kitami, and M. Yokoyama, *J. Solid*

State Chem., 1991, **92**, 537-542.

(22) T. P. Feist, and P. K. Davies, *J. Solid State Chem.,* 1992, **101**, 275-295.

(23) M. R. Allen, A. Thibert, E. M. Sabio, N. D. Browning, D. S. Larsen, and F. E. Osterloh, *Chem. Mater.,* 2010, **22**, 1220-1228.

(24) S. Suzuki, and M. Miyayama, *J. Phys. Chem. B,* 2006, **110**, 4731-4734.

(25) Y. Matsumoto, M. Koinuma, Y. Iwanaga, T. Sato, and S. Ida, *J. Am. Chem. Soc.,* 2009, **131**, 6644-6645.

(26) M. Osada, Y. Ebina, H. Funakubo, S. Yokoyama, T. Kiguchi, K. Takada, and T. Sasaki, *Adv. Mater.,* 2006, **18**, 1023-1027.

(27) K. Momma, and F. Izumi, *J. Appl. Crystallogr.,* 2008, **41***,* 653-658.

(28) S. Kikkawa, S. Takagi, and H. Tamura, *J. Ceram. Soc. Jpn.,* 2008, **116**, 380-383.

(29) T. Taguchi, T. Ozawa, and H. Yashiro, *Phys. Scr.,* 2005, **T115**, 205-206.

(30) N. Jiang, D. Su, and J. C. H. Spence, *Phys. Rev. B,* 2007, **76**, 214117/1-9.

(31) F. Farges, G. E. Brown, and J. J. Rehr, *Phys. Rev. B*, 1997, **56**, 1809-1819.

(32) M. A. Osman, W. R. Caseri, and U. W. Suter, *J. Colloid Interface Sci.*, 1998, **198**, 157-163.

(33) H. Takahashi, M. Kakihana, Y. Yamashita, K. Yoshida, S. Ikeda, M. Hara,

and K. Domen, *Phys. Chem. Chem. Phys.*, 2000, **2**, 4461-4464.

(34) M. Park, H. J. Kim, K. S. Kim, O. W. Duckworth, and S. Komarneni, *J. Phys. Chem. C*, 2012, **116**, 18678-18683.

Figure captions

Figure 1. Crystal structure of K_2TiO_3. Small red spheres: oxide ions; medium blue spheres: titanium ions; large purple spheres: potassium ions. The image was produced based on previous crystallographic data,[17] using the program VESTA.[27]

Figure 2. Photographs of K_2TiO_3 dispersed in acid solution (pH ≤ 1): (a) the initial solution and (b) after 3 days in solution. (c) Tyndall scattering exhibited by the transparent solution shown in (b).

Figure 3. Particle size distributions measured in the light scattering for the colloidal solution over duration time.

Figure 4. TEM image of the K_2TiO_3 colloidal particle dried on copper grid (a), magnified image in the red circle (b), and its electron diffraction pattern (c).

Figure 5. Fourier transforms of Ti K-edge EXAFS spectra for K_2TiO_3 and K_2TiO_3 in nitric acid solution. The vertical dashed lines represent the first and second

peak positions for K_2TiO_3.

Figure 6. Mechanism for the exfoliation of K_2TiO_3 in aqueous nitric acid solution:

(a) parent K_2TiO_3, (b) intermediate state, and (c) exfoliation state.

Figure 1, Y. Masubuchi, et al.

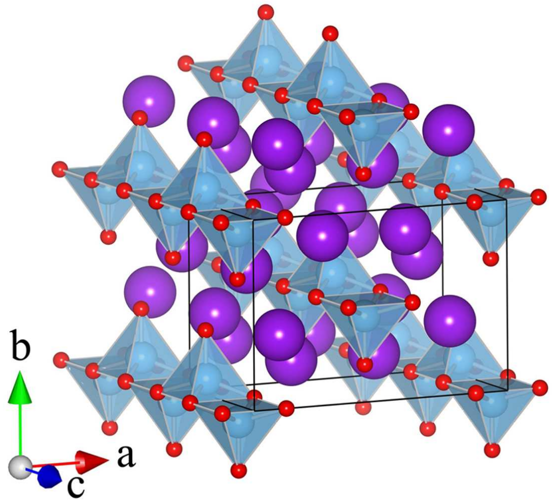

Figure 2, Y. Masubuchi, et al.

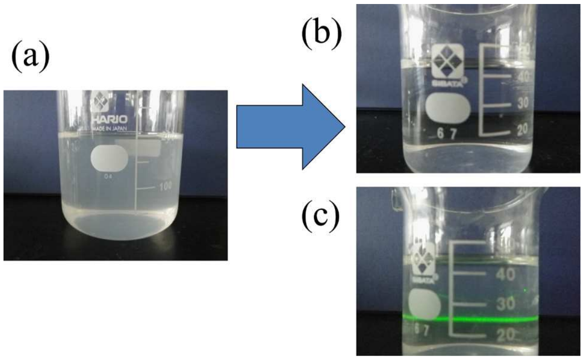

Figure 3, Y. Masubuchi, et al.

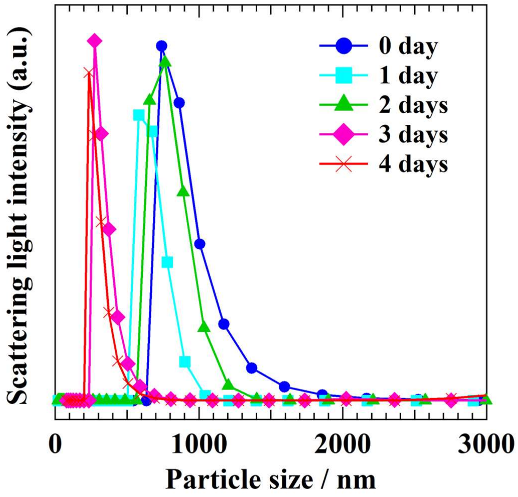

Figure 4, Y. Masubuchi, et al.

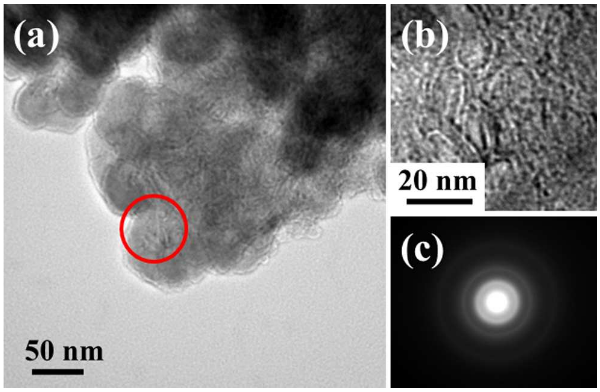

Figure 5, Y. Masubuchi, et al.

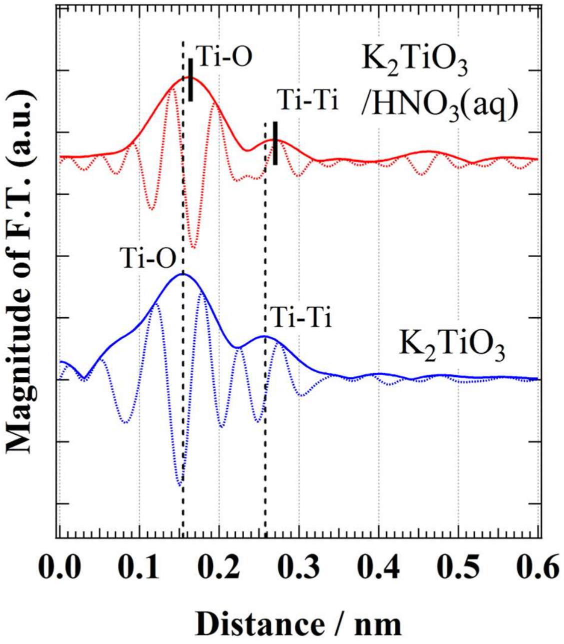

Figure 6, Y. Masubuchi, et al.